

Weierstraß-Institut für Angewandte Analysis und Stochastik

im Forschungsverbund Berlin e.V.

Preprint

ISSN 0946 – 8633

Spinodal dewetting of thin films with large interfacial slip: implications from the dispersion relation

Markus Rauscher ¹ Ralf Blossey ² Andreas Münch ³ Barbara Wagner ⁴

submitted: December 3, 2008

¹ Max-Planck-Institut für Metallforschung,
Heisenbergstr. 3, 70569 Stuttgart, Germany

² Interdisciplinary Research Institute, c/o IEMN Avenue
Poincaré BP 60069, F-59652 Villeneuve d'Ascq, France,

³ School of Mathematical Sciences,
University of Nottingham, NG7 2RD, UK,

⁴ Weierstrass Institute for Applied Analysis and Stochastics (WIAS),
Mohrenstraße 39, D-10117 Berlin

No. 1380
Berlin 2008



2000 *Mathematics Subject Classification.* 35G25, 35K55.

Key words and phrases. thin liquid films, stability, fluid dynamics.

Edited by
Weierstraß-Institut für Angewandte Analysis und Stochastik (WIAS)
Mohrenstraße 39
10117 Berlin
Germany

Fax: + 49 30 2044975
E-Mail: preprint@wias-berlin.de
World Wide Web: <http://www.wias-berlin.de/>

Abstract

We compare the dispersion relations for spinodally dewetting thin liquid films for increasing magnitude of interfacial slip length in the lubrication limit. While the shape of the dispersion relation, in particular the position of the maximum, are equal for no-slip up to moderate slip lengths, the position of the maximum shifts to much larger wavelengths for large slip lengths. Here, we discuss the implications of this fact for recently developed methods to assess the disjoining pressure in spinodally unstable thin films by measuring the shape of the roughness power spectrum. For PS films on OTS covered Si wafers (with slip length $b \approx 1 \mu\text{m}$) we predict a 20% shift of the position of the maximum of the power spectrum which should be detectable in experiments.

1 Introduction

Wetting and dewetting phenomena are not only part of our everyday life but they are particularly relevant to technological applications (e.g., in coating processes) and in biological systems. The dynamics of films of a thickness smaller than 10 or 20 nanometers is not only governed by hydrodynamics, but the finite range of intermolecular forces, which are responsible for the richness of wetting phenomena (1; 2), becomes relevant (3). This is true in particular for spinodally unstable films which have been analysed quantitatively in the framework of the thin-film equation (4). In addition, the quantitative analysis of the roughness power spectrum has been used in order to measure the disjoining pressure (DJP) (or the effective interface potential) between the liquid-solid and the liquid-vapor interface which is a result of the interplay between the interactions among the fluid molecules and the interactions between the fluid and the substrate (5–7).

In the spinodally dewetting systems studied in Refs. (4; 6; 7), i.e., polystyrene (PS) on silicon (Si) wafers covered with a native oxide layer, hydrodynamic slip between the fluid and the solid substrate could be neglected. However, recently, the slip length of PS on octadecyltrichlorosilane (OTS) and decyltrichlorosilane (DTS) coated Si wafers was discovered to range up to the scale of a micron (8–11). The dewetting patterns, in particular the shape of the dewetting rims around the growing holes in the film were analyzed using a thin-film equation valid in the regime of large slip lengths, the so-called strong-slip model, (8; 12). The thickness of the films was on the order of a few 100 nm and the dewetting mechanism was therefore nucleation rather than spinodal. However, since the hydrodynamic boundary conditions influence the rim shape it is to be expected that the power spectrum of spinodally unstable films is affected as well. Some dependencies of the dominant wavelength and time

scale on the magnitude of the slip length for the case of an attracting van der Waals potential are discussed in (13). In this study, we systematically compare thin spinodally dewetting films with zero to large large slip lengths. Our main motivation is the availability of experimental systems (PS on OTS or DTS-covered Si wafers (8–11)) which exhibit extremely large slip lengths and against which we can test our theoretical analysis in order to not only infer qualitative but also quantitative results. In particular, we consider an effective interface potential calculated from Hamaker constants as given in (7).

In the following Sec. 2 we first compare the dispersion relations for lubrication models for zero to moderate slip lengths with the dispersion relation for the regime of large slip lengths. We establish that even though the energetics is the same, films dewetting for large slip lengths have a qualitatively different dispersion relation as compared to sticky films, and therefore their structure factor has a maximum at a different wavenumber. We investigate the relevance of the difference between the dispersion relations for the sample systems PS on Si and on OTS(DTS)-covered Si in Sec. 3 and conclude in Sec. 4.

For clarity of presentation we restrict our analysis to one-dimensional interfaces. The generalization to real two-dimensional interfaces is straightforward for the lubrication models for zero to moderate slip. The generalization of the lubrication model for large slip is not completely obvious due to the appearance of additional cross-terms and we have included it here in an appendix (14). We note that omission of these cross-terms would be discovered at the level of the dispersion relation, where the growth rate would not only depend on the modulus of the wave vector but also on its direction, in contradiction to the isotropy of the physical situation. For all slip regimes we obtain the same dispersion relation for two-dimensional interfaces as for the corresponding problem with one-dimensional interfaces, except that the wavenumber is now replaced by the absolute value of the wave vector.

2 Spinodal dewetting

2.1 The no-, weak-, and intermediate slip limit

If the slip length b is small compared to the lateral length scale L in the dewetting film (i.e., the spinodal wavelength, see below), or comparable to L , the dynamics of a thin non-volatile Newtonian liquid film between a vapour of negligible viscosity and density, and an impermeable substrate is given in the lubrication approximation (i.e., for $\varepsilon = H/L \ll 1$, with the mean film thickness H) by a degenerate parabolic partial differential equation of fourth order for the film thickness $h(x, t)$ (3)

$$\partial_t h = -\partial_x \{M(h) \partial_x [\Pi(h) + \sigma \partial_x^2 h]\} \quad (2.1)$$

with the surface tension of the liquid-vapour interface σ , and the disjoining pressure (DJP) $\Pi(h) = -\partial_h \Phi(h)$ (the negative derivative with respect to the film thickness of the effective interface potential) (1; 2). If the slip length is on the order of H or smaller, the so-called weak-slip regime, the mobility factor is given by $M(h) = (h^3/3 + b h^2)/\eta$, with the fluid viscosity η . For $b \sim L$,

we have $M(h) = b h^2 / \eta$, called the intermediate-slip regime. The well-known no-slip regime is reached by taking the limit $b \rightarrow 0$ in the weak-slip regime, leading to $M(h) = h^3 / (3\eta)$, see (12) for more details.

A homogeneous flat film of thickness H is linearly unstable if $\partial_h^2 \omega(H) = -\partial_h \Pi(H) < 0$: In the early regime of dewetting, we can linearize Eq. (2.1) about the base state H . For small perturbations $\delta h(x, t) = H - h(x, t)$ we get

$$\partial_t \delta h = -M(H) \partial_x^2 [\partial_h \Pi(H) + \sigma \partial_x^2 \delta h]. \quad (2.2)$$

The ansatz $\delta h(x, t) = \delta h(q, t) \exp(i q x)$ corresponds to a Fourier transformation with respect to x and leads to solutions of the form $\delta h(q, t) = \delta h(q, 0) \exp[\omega(q) t]$ with the dispersion relation

$$\begin{aligned} \omega(k) &= M(H) q^2 [\partial_h \Pi(H) - \sigma q^2] \\ &= \frac{1}{T} (q/Q)^2 [2 - (q/Q)^2]. \end{aligned} \quad (2.3)$$

For unstable films, i.e., for $\partial_h \Pi(H) > 0$, there is a band of unstable modes with wave number $0 < q < q_c$, with $q_c = \sqrt{[\partial_h \Pi(H)] / \sigma}$. The dispersion relation has a maximum at $Q = q_c / \sqrt{2}$, which also defines the typical lateral length scale $L = 2\pi / Q$ which is also called the spinodal wavelength. The typical time scale, i.e., the inverse growth rate of the fastest growing mode, is given by $T = 1 / [\sigma M(H) Q^4]$.

The dispersion relation $\omega(q)$ has the form given in Eq. (2.3) in the no-slip regime, in the weak-slip, as well as in the intermediate-slip regime. For $b \lesssim L$ changing the slip length therefore only changes the time scale T but not the position Q of the maximum of $\omega(q)$. Q , on the other hand, is only determined by the ratio of $\partial_h \Pi(H)$ and σ . If one knows σ , measuring the position of the maximum of $\omega(q)$ for a number of film thicknesses allows to determine $\partial_h \Pi(h)$ and therefore the effective interface potential $\Phi(h)$ (6; 7). This has been accomplished experimentally by measuring the power spectrum of the surface roughness $S(q, t) = |\delta h(q, t)|^2$, which, in turn, can be calculated from the initial spectrum $S(q, 0) = |\delta h(q, 0)|^2$ and the dispersion relation $\omega(q)$

$$S(q, t) = S(q, 0) \exp[2\omega(q) t]. \quad (2.4)$$

If $S(q, 0)$ is flat in the range of unstable modes, then $S(q, t)$ has a maximum at the same position as $\omega(q)$, i.e., at $q = Q$.

2.2 Strong-slip limit

For the case of a slip length b much larger than L , the thin film evolution can be captured by a different thin film model (12; 13), called the strong-slip model by Münch et al. (12). It can be written as

$$\begin{aligned} \eta u &= 4b\eta \partial_x (h \partial_x u) + b h \partial_x [\Pi(h) + \partial_x^2 h] \\ &\quad - b h \rho (\partial_t u + u \partial_x u) \end{aligned} \quad (2.5a)$$

$$\partial_t h = -\partial_x (h u), \quad (2.5b)$$

with the fluid mass density ρ and the horizontal flow velocity $u(x, t)$. We note that this model is associated with plug flow in the cross-section. For the experimental systems considered here we are not interested in the last term in Eq. (2.5a) since the inertial term proportional to ρ is negligible. However, for completeness, we calculate the dispersion relation including this term. The first term on the right hand side of Eq. (2.5a) is proportional to the divergence of the total longitudinal shear stress component parallel to the substrate. Note that the velocity u cannot be eliminated from Eq. (2.5) even if the inertial term is neglected.

If we perturb Eq. (2.5) about a resting $[u(x, 0) = 0]$ flat film of thickness H we get to first order in the perturbation the problem

$$\begin{aligned} \eta \delta u = & 4 b H \eta \partial_x^2 \delta u + b H \partial_x [\partial_h \Pi(H) \delta h + \partial_x^2 \delta h] \\ & - b H \rho \partial_t \delta u \end{aligned} \quad (2.6a)$$

$$\partial_t \delta h = - H \partial_x \delta u. \quad (2.6b)$$

With the normal modes ansatz $\delta h(q, t) = \delta h(q, 0) \exp [\omega(q) t + i q x]$ and $\delta u(q, t) = \delta u(q, 0) \exp [\omega(q) t + i q x]$ we get, after taking the derivative of Eq. (2.6b) with respect to x and subsequently eliminating $\delta h(q, 0)$, a quadratic equation for the dispersion relation $\omega(q)$

$$\begin{aligned} \eta \omega(q) = & - 4 b H \eta q^2 \omega(q) + b H^2 q^2 [\partial_h \Pi(H) - \sigma q^2] \\ & - b H \rho [\omega(q)]^2 \end{aligned} \quad (2.7)$$

with the two solutions

$$\begin{aligned} \omega_{1/2}(q) = & -\frac{\eta}{2\rho} \left(4q^2 + \frac{1}{bH} \right) \\ & \times \left[1 \pm \sqrt{1 + \frac{H q^2 [\partial_h \Pi(H) - \sigma q^2]}{\frac{\eta^2}{\rho} (4q^2 + \frac{1}{bH})}} \right]. \end{aligned} \quad (2.8)$$

While the first solution $\omega_1(q)$, corresponding to the plus sign in Eq. (2.8), is negative for all q and does therefore not contribute significantly to the roughness spectrum, the second solution $\omega_2(q)$ is zero for $q^2 [\partial_h \Pi(H) - \sigma q^2] = 0$, i.e., for $q = 0$ and for $q = q_c = \sqrt{2} Q$. For sufficiently small ρ or sufficiently large b the term under the square root is negative for large enough $q > q_c$. The corresponding modes oscillate in time. However, their real part is given by $\text{Re } \omega_2(q) = -\eta [4q^2 + 1/(bH)] / (2\rho) < 0$ and thus, these modes are heavily damped.

If inertia is negligible we can ignore the last term proportional to ρ in Eq. (2.7) (or take the limit $\rho \rightarrow 0$ in Eq. (2.7)) and we get

$$\begin{aligned} \omega(q) = & \frac{b H^2 q^2 [\partial_h \Pi(H) - \sigma q^2]}{\eta (1 + 4 b H q^2)} \\ = & \frac{(q/Q)^2 [2 - (q/Q)^2]}{T [1 + B (q/Q)^2]}, \end{aligned} \quad (2.9)$$

with the time scale $T = \eta / (\sigma b H^2 Q^4)$, as in the intermediate-slip regime. As expected, taking the limit $B \rightarrow 0$ ($b \rightarrow 0$) we recover the dispersion relation of the intermediate-slip model. As compared to Eq. (2.3), we have one additional dimensionless parameter $B = 4 b H Q^2$ determining the relevance of slip, which is of order unity in the strong-slip limit discussed here. Both the time scale T as well as B depend on the slip length. Introducing the b -independent time scale $T' = B T = 4 \eta / (\sigma H Q^2)$ we can study the dependence of the dispersion relation on the slip length more easily. In the strong-slip model, neither T nor T' are the inverse of the maximum of the dispersion relation. Since the numerator in Eq. (2.9) is proportional to the dispersion relation of the weak- and no-slip models discussed in the previous section and since the denominator is positive, the strong slip model has the same band of unstable modes $q < q_c$. Taking the derivative of Eq. (2.9) we get the position q_{\max} of the maximum of $\omega(q)$ at

$$q_{\max} = Q \sqrt{\frac{\sqrt{1 + 2B} - 1}{B}}. \quad (2.10)$$

Fig. 1 shows the dispersion relation for the strong-slip regime for various values of B . For $B \rightarrow 0$ we recover the shape of the dispersion relation for the weak and intermediate slip regime, but the time scale T diverges in this limit. For increasing B the location q_{\max} of the maximum moves to smaller values of q and the height of the maximum $\omega(q_{\max})$ approaches $2/T'$ from below. In the limit $B \rightarrow \infty$ we get $\omega(q) \rightarrow [2 - (q/Q)^2] / T'$.

3 Experimental relevance

In the experiments discussed in (6) the shift of Q with the film thickness was used to determine the effective interface potential $\Phi(z)$, assuming the dispersion relation in Eq. (2.3), i.e., for the weak/intermediate slip regime. The surface tension coefficient was $\sigma = 31$ mN/m and the DJP had the form $\Pi(z) = -A / (6 \pi z^3)$, with the Hamaker constant 2.2×10^{-20} Nm. From this we get for the dimensionless slip length $B = 0.23 \text{ nm}^2 b / H^3$. Therefore, in order to have, e.g., $B > 1$ or $B > 0.1$ for the lowest film thickness $H = 2$ nm in the experiment, b has to be larger than 35 nm and 3.5 nm, respectively.

The position of the peak in the power spectrum as a function of H and b normalized to the position in the weak/intermediate slip model that one would observe for the material combination studied in (6) is shown in Fig. 2. Clearly, the shift in the peak is larger for smaller film thicknesses H and larger slip length b . In order to get a deviation of the peak position on the order of 5% for the smallest film thicknesses of $H = 2$ nm, the slip length has to be larger than 8 nm, i.e., much larger than expected for PS on Si.

If, on the other hand, the strong-slip regime was to apply and one tried to determine $\partial_h \Pi$ from the measured peak position q_{\max} [see Eq. (2.10)] with the equation valid only in the weak and intermediate slip regime, i.e., $q_{\max} = \sqrt{\partial_h \Pi^* / (2 \sigma)}$ with an “apparent” DJP Π^* , one would produce a systematic error in the measurement. The ratio of the actual DJP $\partial_h \Pi$ and the “apparent”

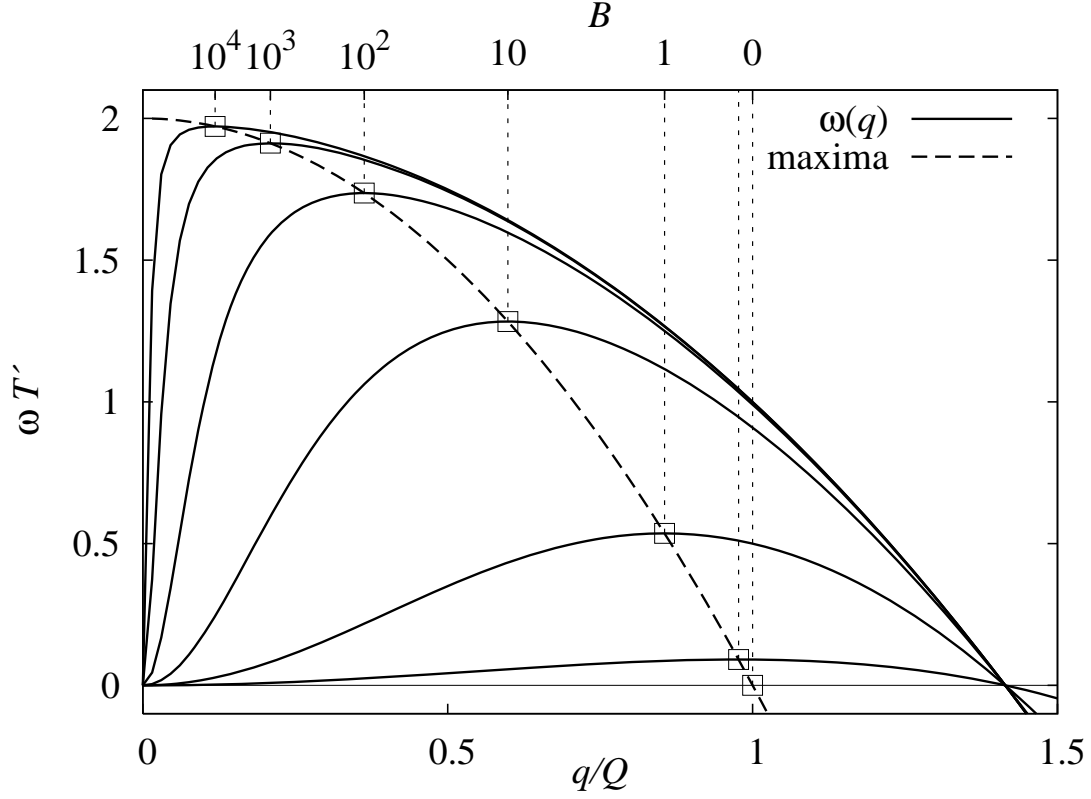


Figure 1: Dispersion relation in the strong slip limit in Eq. (2.9) (full lines) for various values of B (see upper axis ticks). The location of the maximum of the dispersion relation shifts to smaller values q/Q and the height approaches $2/T'$ from below for increasing B (dashed line).

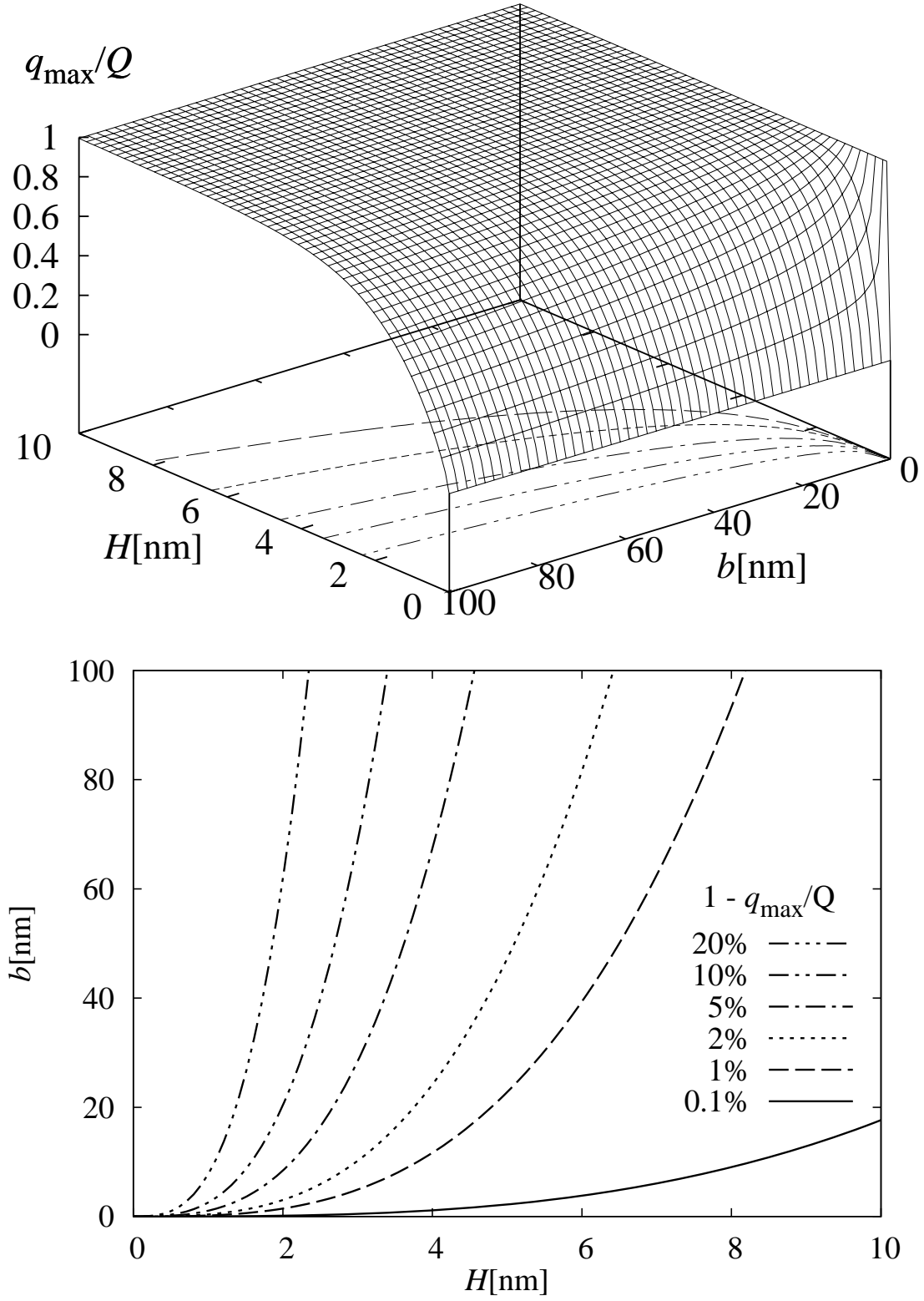


Figure 2: Shift of the position of the maximum q_{\max} of the dispersion relation $\omega(q)$ as compared to the position expected for the weak and intermediate slip model and experimental parameters from (6) as a function of the film thickness H and the slip length b . The contour lines indicate the slip length b necessary in order to obtain a deviation of 0.1%, 1%, 5%, 10%, and 20%.

DJP $\partial_h \Pi^*$ is obtained by squaring Eq. (2.10)

$$\partial_h \Pi^*(H) = \frac{\sqrt{1+2B}-1}{B} \partial_h \Pi(H). \quad (3.1)$$

In order to get a first estimate on the error we assume that only non-retarded dispersion forces are relevant and get to first order in B

$$\partial_h \Pi^*(H) \approx \frac{A}{2\pi H^4} - \frac{A^2 b}{4\pi^2 \sigma H^7}. \quad (3.2)$$

Therefore, a spurious subleading term $\propto 1/z^5$ is generated in the “apparent” effective interface potential $\Phi^*(z) = -\int^z \Pi^*(z') dz'$.

The system considered in (6), i.e., PS on a Si wafer covered with a native oxide layer, is known not to exhibit significant slip. However, recently it has been demonstrated, that covering the same wafer with an OTS or DTS brush leads to very large slip lengths up to the order of microns (8–10). With the material parameters of OTS, SiO, and Si together with the thickness of the OTS layer and of the SiO layer in (8) we calculate the effective interface potential for a PS film on an OTS covered Si wafer using Eq. (3) in Ref. (7). With this, we can calculate the deviation of the position of the maximum of the dispersion relation q_{\max} from the position in the weak-slip limit Q as shown in Fig. 3. With a film thickness of 4 nm a slip length of $b = 1 \mu\text{m}$ is enough to generate a 20% shift in the maximum of the dispersion relation. Such a large shift should be detectable in the experiments.

4 Conclusions

In this paper we demonstrated that the hydrodynamic boundary condition at the substrate surface significantly changes the power spectrum of film thickness variations in spinodal dewetting for experimentally relevant systems. Analysing only the peak position without knowledge of the hydrodynamic boundary conditions can lead to significant systematic errors in the data analysis. As pointed out in (15), viscoelastic thin films show a similar behaviour: while the position of the maximum of the dispersion relation is identical to the position in the Newtonian weak-/intermediate-slip case, in the strong-slip case it shifts to smaller wave numbers for increasing slip length (15–17).

The power spectrum of capillary waves should be affected by hydrodynamic slip as well. However, up to now, a stochastic version of the thin-film equation is available only for substrates without slip (18; 19) and the phenomenological ansatz taken in (20) can be extended directly to the case of weak- and intermediate-slip only. In the case of vanishing slip the position of the maximum of the power spectrum approaches Q from above as time proceeds (21). Since the no-slip, the weak-slip, and the intermediate-slip case differ only in the mobility factor M , the same behaviour can be expected for the weak and intermediate-slip case. The mechanism for this noise-induced coarsening is simple: thermal fluctuations generate short wavelength fluctuations rather rapidly before the instability sets in, amplifying modes with larger wavelength. In the strong slip case, the maximum of the dispersion relation

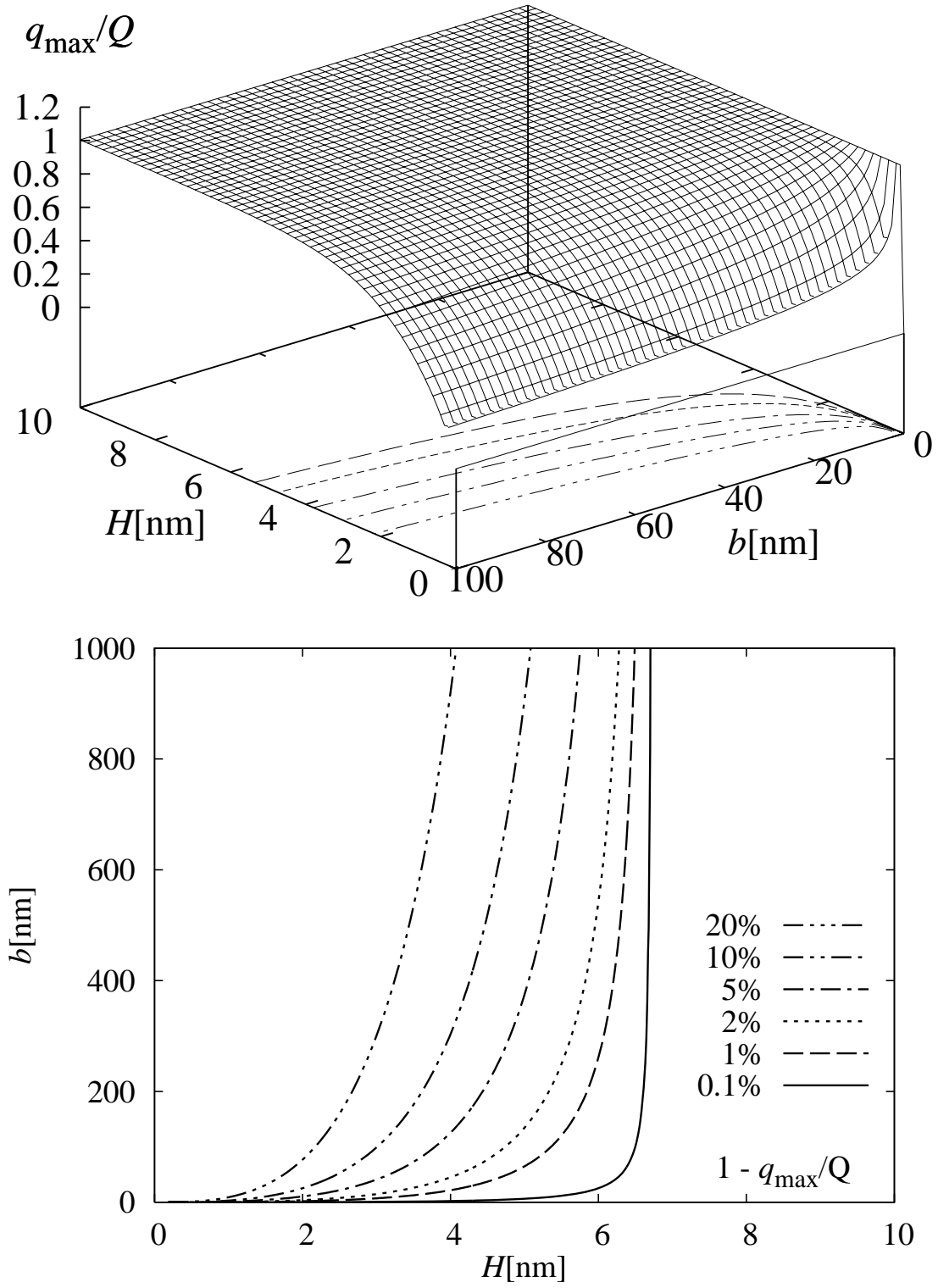


Figure 3: Shift of the position of the maximum q_{\max} of the dispersion relation $\omega(q)$ as compared to the position expected for the weak and intermediate slip model and experimental parameters for a PS film on OTS from (7) as a function of the film thickness H and the slip length b . The contour lines indicate the slip length b necessary in order to obtain a deviation of 0.1%, 1%, 5%, 10%, and 20%.

shifts to very large wavelengths for increasing b , which could emphasize the effect of noise-induced coarsening. However, a detailed analysis of a stochastic strong-slip thin-film equation is needed to reach a conclusion on this point.

Acknowledgement

The authors thank K. Jacobs for inspiring discussions. A.M., B.W., and M.R. acknowledge funding from DFG priority program SPP 1164 “Nano- and Microfluidics”.

Appendix

The generalization of the strong-slip model to 3D has been derived in (14). With the two lateral velocity components u and v in the x and y -direction, respectively, the model equations in non-dimensional form are

$$\begin{aligned} \text{Re} \frac{du}{dt} = & \frac{1}{h} [\partial_x (4h\partial_x u + 2h\partial_y v) + \partial_y (h\partial_x v + h\partial_y u)] \\ & + \partial_x [\Delta h + \Pi(h)] - \frac{u}{h\beta} \end{aligned} \quad (.1a)$$

$$\begin{aligned} \text{Re} \frac{dv}{dt} = & \frac{1}{h} [\partial_y (4h\partial_y v + 2h\partial_x u) + \partial_x (h\partial_x v + h\partial_y u)] \\ & + \partial_y [\Delta h + \Pi(h)] - \frac{v}{h\beta} \end{aligned} \quad (.1b)$$

$$\partial_t h = -\partial_x (h u) - \partial_y (h v). \quad (.1c)$$

Here, we abbreviate the total/materials derivative $d/dt = \partial_t + u\partial_x + v\partial_y$ and the two-dimensional Laplace operator $\Delta = \partial_x^2 + \partial_y^2$ and Re is the Reynolds number. The lateral length scale L , the vertical length scale H , and the time scale T have been introduced in the main text. For this model the slip length is large and of order $b = \beta/\varepsilon^2$, where β is an $O(1)$ constant. The scale for the (disjoining) pressure is $P = \eta/T$. The capillary number is $\text{Ca} = \eta L/(\sigma T) = \varepsilon$.

The linear stability of a flat film is again a straightforward calculation, by taking the first order in the perturbation, the problem for $u = \delta u$, $v = \delta v$ and $h = H + \delta h$ and making the normal modes ansatz $(\delta u, \delta v, \delta h)(\vec{q}, t) = (\delta u(\vec{q}, 0), \delta v(\vec{q}, 0), \delta h(\vec{q}, 0)) \exp[\omega(\vec{q})t + i\vec{q} \cdot \vec{r}]$, with $\vec{q} = (q_x, q_y)$ and $\vec{r} = (x, y)$.

Abbreviating $\delta u(\vec{q}, 0) = \delta u_0$, $\delta v(\vec{q}, 0) = \delta v_0$, $\delta h(\vec{q}, 0) = \delta h_0$, we obtain the linear eigenvalue problem

$$\begin{aligned} \eta \delta u_0 = & -b\eta H [(4q_x^2 + q_y^2) \delta u_0 + 3q_x q_y \delta v_0] \\ & + i b H q_x [\partial_H \Pi(H) - \sigma q^2] \delta h_0 \end{aligned} \quad (.2a)$$

$$\begin{aligned} \eta \delta v_0 = & -b\eta H [(4q_y^2 + q_x^2) \delta v_0 + 3q_x q_y \delta u_0] \\ & + i b H q_y [\partial_H \Pi(H) - \sigma q^2] \delta h_0 \end{aligned} \quad (.2b)$$

$$\omega(\vec{q}) \delta h_0 = -i H (q_x \delta u_0 + q_y \delta v_0), \quad (.2c)$$

with $q^2 = |\vec{q}|^2$. Here, we have neglected the contributions from the inertial terms and we have switched to dimensional quantities in order to connect to

the main body of the article. From (.2) we find the same dispersion relation as we obtained for the 2D case in (2.9), i.e., $\omega(\vec{q}) = \omega(q)$, by setting the determinant of the matrix corresponding to the linear system to zero and by solving for $\omega(q)$. Alternatively, one can determine $q_x \delta u_0 + q_y \delta v_0$ from Eqs. (.2a) and (.2b) which yields

$$(q_x \delta u_0 + q_y \delta v_0) (1 + 4 b H q^2) = \frac{i b H}{\eta} q^2 [\partial_H \Pi(H) - \sigma q^2] \delta h_0. \quad (.3)$$

Inserting this in Eq. (.2c) we recover Eq. (2.9).

References

- [1] de Gennes, P. G. *Rev. Mod. Phys.* **1985**, *57*, 827–860.
- [2] Dietrich, S. Wetting Phenomena. In *Phase Transitions and Critical Phenomena*; Domb, C., Lebowitz, J. L., Eds.; Academic Press: London, 1988; Vol. 12, Chapter 1, pp 1–218.
- [3] Oron, A.; Davis, S. H.; Bankoff, S. G. *Rev. Mod. Phys.* **1997**, *69*, 931–980.
- [4] Becker, J.; Grün, G.; Seemann, R.; Mantz, H.; Jacobs, K.; Mecke, K. R.; Blossey, R. *Nature Materials* **2003**, *2*, 59–63, [dx.doi.org/10.1038/nmat788](https://doi.org/10.1038/nmat788).
- [5] Bischof, J.; Scherer, D.; Herminghaus, S.; Leiderer, P. *Phys. Rev. Lett.* **1996**, *77*, 1536–1539.
- [6] Seemann, R.; Herminghaus, S.; Jacobs, K. *Phys. Rev. Lett.* **2001**, *86*, 5534–5537.
- [7] Seemann, R.; Herminghaus, S.; Jacobs, K. *J. Phys.: Condens. Matter* **2001**, *13*, 4925–4938.
- [8] Fetzer, R.; Jacobs, K.; Münch, A.; Wagner, B.; Witelski, T. P. *Phys. Rev. Lett.* **2005**, *95*, 127801.
- [9] Fetzer, R.; Rauscher, M.; Münch, A.; Wagner, B. A.; Jacobs, K. *Europhys. Lett.* **2006**, *75*, 638–644, [cond-mat/0603452](https://arxiv.org/abs/cond-mat/0603452).
- [10] Fetzer, R.; Münch, A.; Wagner, B.; Rauscher, M.; Jacobs, K. *Langmuir* **2007**, *23*, 10559–10566.
- [11] Fetzer, R.; Jacobs, K. *Langmuir* **2007**, *23*, 11617–11622.
- [12] Münch, A.; Wagner, B.; Witelski, T. *J. Eng. Math.* **2005**, *53*, 359–383.
- [13] Kargupta, K.; Sharma, A.; Khanna, R. *Langmuir* **2004**, *20*, 244–253.

- [14] Münch, A.; Wagner, B. Contact-line instability of dewetting film for large slip, (in preparation).
- [15] Blossey, R.; Münch, A.; Rauscher, M.; Wagner, B. *Eur. Phys. J. E* **2006**, *20*, 267–271, cond-mat/0604085.
- [16] Rauscher, M.; Münch, A.; Wagner, B.; Blossey, R. *Eur. Phys. J. E* **2005**, *17*, 373–379.
- [17] Münch, A.; Wagner, B.; Rauscher, M.; Blossey, R. *Eur. Phys. J. E* **2006**, *20*, 365–368.
- [18] Mecke, K.; Rauscher, M. *J. Phys.: Condens. Matter* **2005**, *17*, S3515–S3522, proceedings of the 6th Liquid Matter Conference.
- [19] Grün, G.; Mecke, K. R.; Rauscher, M. *J. Stat. Phys.* **2006**, *122*, 1261–1291.
- [20] Davidovitch, B.; Moro, E.; Stone, H. A. *Phys. Rev. Lett.* **2005**, *95*, 244505, cond-mat/0509803.
- [21] Fetzer, R.; Rauscher, M.; Seemann, R.; Jacobs, K.; Mecke, K. *Phys. Rev. Lett.* **2007**, *99*, 114503, arXiv:0706.1895.